

# Post Stall Studies of Untwisted Varying Aspect Ratio Blades with an NACA 4415 Airfoil Section – Part I.

C. Ostowari (1) and D. Naik (2).

Aerospace Engineering Department, Texas A&M University, College Station, Texas 77843, U.S.A.

## ABSTRACT

Wind turbine blades operate over a wide angle of attack range. Unlike aircraft, a wind turbine's angle of attack range extends deep into stall where the three dimensional performance characteristics of airfoils are not generally known. Peak power predictions upon which wind turbine components are sized, depend on a good understanding of a blade's post stall characteristics.

Part I of this paper documents results of the wind tunnel investigation of untwisted, constant chord blades having four aspect ratios, with an NACA 4415 series airfoil section, at angles of attack ranging from  $-10$  to  $110$  degrees. Tests were conducted for aspect ratios of 6, 9, 12 and infinity at four Reynolds numbers ranging from one-quarter million to one million. Part II of this paper will discuss results on the same family of airfoil section but with varying thickness ratios.

Results of force and pitching moment measurements, over the angle of attack range, for all combinations of Reynolds numbers and aspect ratios, and the effects of boundary layer tripping, have been presented.

Both initial and secondary stall are presented. The maximum drag coefficient is found to occur at an angle of attack of  $90$  degrees. The pitching moment is unstable beyond stall. The lift and post-stall drag coefficients decrease with decreasing aspect ratio. The boundary layer tripping is observed to decrease the lift curve slope and stalling angle of attack. The drag coefficient (with tripping) is significantly affected only at low aspect ratio. Beyond secondary stall, the lift to drag ratio is independent of aspect ratio. The maximum lift to drag ratio for the infinite aspect ratio blade is roughly twice that of the blade with an aspect ratio of six. This effect is independent of Reynolds number in the range studied.

## SYMBOLS

The force and moment data have been referred to the quarter-chord location on the airfoil. Dimensional quantities are given in SI units. Measurements were made in U.S. Customary Units. The symbols used herein are defined as follows:

AR	Aspect ratio
b	Span
c	Airfoil reference chord
$C_D$	Drag coefficient = Drag/(dynamic pressure x area)
$C_L$	Lift coefficient = Lift/(dynamic pressure x area)
$C_M$	Pitching moment coefficient with respect to the 0.25 c location = Moment/(dynamic pressure x area x c)
M	Mach number
q	Dynamic pressure
RN	Reynolds number
S	Reference area (surface area)
$\alpha$	Angle of attack

(1). Assistant Professor.

(2). Graduate Research Assistant.

**INTRODUCTION**

Current research efforts are directed towards the design of cost effective wind energy conversion devices. The accomplishment of this goal requires good rotor-to-load matching. Proper matching is dependent on an accurate knowledge of the post-stall airfoil characteristics, upon which the peak power predictions are strongly dependent.

Contemporary wind turbine blades are typically of high aspect ratio for cost effective, high RPM operation. The blade sections are subjected to a large range of angles of attack for which, particularly at post stall conditions, aerodynamic data is lacking. This paper attempts to fill part of this airfoil data void and presents the post-stall aerodynamic characteristics as a function of aspect ratio and Reynolds number. Many two-dimensional studies have been done on blades. Examples are the studies on uncambered airfoils done by Michos *et al.* (Ref. 1) and the studies on cambered airfoils, like the GA(W) series (Ref. 2). The present work is a study of three dimensional blades with cambered airfoils. Aspect ratios of 6, 9, 12 and infinity were tested using constant chord blades over the angle of attack range of -10 to 110 degrees. The airfoil section used in the study was NACA 4415. The tests were conducted for Reynolds numbers (with respect to blade chord) of  $0.25 \times 10^6$ ,  $0.50 \times 10^6$ ,  $0.75 \times 10^6$  and  $1.0 \times 10^6$ .

Also presented is the effect of boundary layer tripping on the aerodynamic characteristics. This was achieved through the application of chart tape at selected chord locations on the blade upper and lower surface. This roughly simulates an unclean blade that has been struck by insects, grit and bird droppings.

The tests were conducted at the Texas A&M University Low Speed Wind Tunnel Facility. The blade performance characteristics presented here are mainly lift coefficient and drag coefficient along with some pitching moment data versus angle of attack.

**EXPERIMENTAL SET-UP**

**Wind Tunnel Description:**

The Texas A&M 2.13 m x 3.05 m Low Speed Wind Tunnel is a closed circuit, single return type tunnel with an atmospheric test section. A schematic of the wind tunnel is given in Figure 1. The main blance of the tunnel is a six component, pyramidal, virtual center external balance. The resolution of the various instrumentation systems is given in Table I. A Perkin-Elmer 8/16 E minicomputer was used for data acquisition and for reduction of final data and plots.

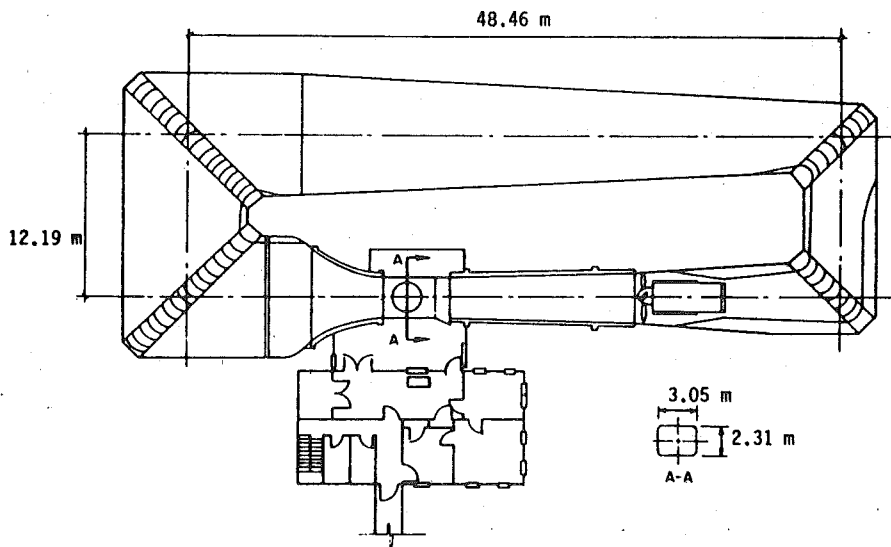


Figure 1 Schematic of the Texas A&M University 2.31 x 3.05 Low Speed Wind Tunnel

Table I Instrument Resolution

Measurement	Resolution		
	Dimensional form	Coefficient form*	
		probable	maximum
lift (balance)	$\pm 1.78$ N	$\pm 0.0002$	$\pm 0.0034$
drag (balance)	$\pm 0.89$ N	$\pm 0.0001$	$\pm 0.0017$
pitching moment (balance)	$\pm 0.27$ Nm	$\pm 0.00003$	$\pm 0.0005$
angle of attack	$\pm 0.1^\circ$	---	---
dynamic pressure	$\pm 0.4\%$	---	---

\*For infinite aspect ratio blades.

#### Model Description:

The model used was of the reflection plane type. This provides an effective aspect ratio that is twice the model aspect ratio. The coordinates of the model's NACA 4415 airfoil section are given in Reference 3. The model extended into the tunnel section from an external-balance mount that was flush with the tunnel floor (Figure 2).

The two dimensional model was sized with a 2.13 m span and a 0.305 m chord. This corresponds to a blade with infinite aspect ratio when placed in the 2.13 m x 3.05 m tunnel section. Effective aspect ratios of 12, 9 and 6 were obtained by cutting the model at appropriate span locations. Angle of attack variation was achieved through rotation of the turntable that is built into the tunnel floor. This turntable rotates with the external balance but is isolated from it. For boundary layer trip studies, the models were fitted with transition strips located at 5% chord on the upper surface and at 10% chord on the lower surface. The transition strips consisted of two layers of 0.127 mm thick and 2.36 mm wide chart tape. The trip height is based on the critical height necessary to trip the boundary layer as given by Reference 4.

The model was fabricated from 12.7 mm douglas-fir vertical laminates bonded with wood glue. The blade lower end was shaped to facilitate attachment to the balance mount. Care was taken to ensure that this bulge did not protrude into the tunnel section. Further, the 0.25 chord location was used as a reference point for model mounting. This was done to minimize the error in moment transfer.

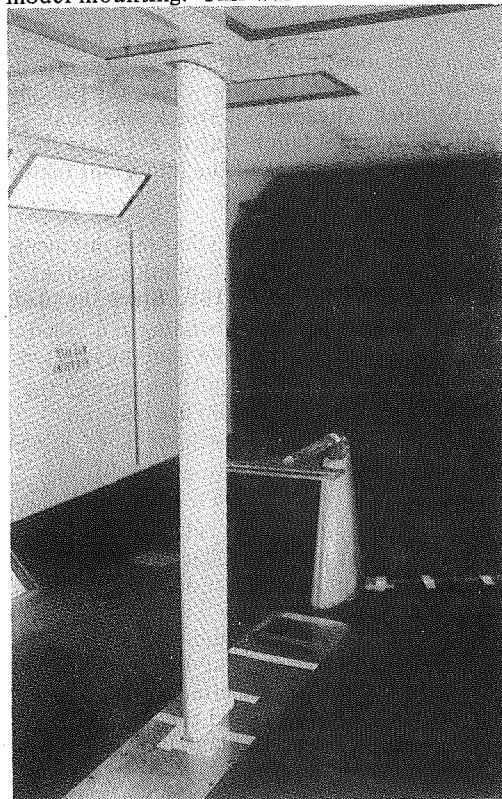


Figure 2 Untwisted Blade Model Mounted in the Wind Tunnel Test Section

## POST STALL STUDIES

### TEST PROCEDURE

#### Test Conditions:

The four Reynolds numbers, along with corresponding dynamic pressures and Mach numbers, at which the models were tested are given in Table II.

Table II Test Conditions

Reynolds Number* ( $\times 10^6$ )	Dynamic pressure ( $N/m^2$ )	Mach number
0.25	71.82	0.05
0.50	277.70	0.09
0.75	627.23	0.14
1.00	1110.82	0.19

\*The Reynolds number is based on the airfoil chord length.

#### Procedure:

Force and moment measurements were made for 7 blade configurations (4 aspect ratios, 3 with trip-strips) at the four different Reynolds numbers given in Table II and for angles of attack ranging from  $-10^\circ$  to  $110^\circ$ . The three component force measurements were made using the wind tunnel main balance system. Further, section drag measurements were made with the wake rake apparatus for all four infinite aspect ratio blades. Wake rake surveys were made at four different Reynolds number with the angle of attack ranging from  $-10^\circ$  to  $12^\circ$  in  $2^\circ$  increments. The wake rake was located one chord length behind the model trailing edge.

The difference between the force balance drag measurement and wake rake drag estimate is the end-plate and interference drag with the tunnel floor and ceiling which depend upon both the lift coefficient and the section geometry. The wake survey method cannot be utilized when flow separation is present. For this reason it was not applied to high angles of attack. However, under high drag conditions, the end-plate tare and interference tare is a relatively small portion of the total drag. Therefore, the tare curve is extrapolated for high lift coefficient conditions and is generally assumed constant past a lift coefficient of roughly 1.3.

All data were corrected for tunnel-wall effects (wake blockage, solid blockage, buoyancy drag, etc.) using the standard procedure given in Reference 4.

### RESULTS AND DISCUSSION

The reduced data is presented in the form of plots of lift coefficient, drag coefficient, and pitching moment coefficient versus angle of attack. In some cases, the full angle of attack range ( $-10^\circ$  to  $110^\circ$ ) is not presented. The angle of attack range was restricted to prevent the longer blades from structural failure due to excessive loading, especially at combinations of high AR and high RN. Some of the important features of the force balance data are discussed below.

**Reynolds Number Effect:** Results of lift, drag and pitching moment measurements are shown in Figure 3, for a blade of infinite aspect ratio, for a Reynolds number range of  $0.25 \times 10^6$  to  $1.0 \times 10^6$ .  $C_{Lmax}$  of 1.4 occurs at  $\alpha = 18^\circ$ . Since the blade was only supported at one end (Figure 2), a certain amount of bending and twisting occurred at high RN and high  $C_L$  conditions. The effect of blade bending and twisting is to produce a somewhat finite wing, which affects the circulation around the wing and causes some loss of lift while increasing the drag. There has been no attempt to correct either  $C_{Lmax}$  or the lift curve slope for this effect. Thus, as can be seen in Figure 3(a),  $C_{Lmax}$  decreases with increasing RN. For a true 2-D section the trend would have been reversed (Reference 3). The  $RN = 1.00 \times 10^6$  curve in Figure 3(a) shows premature stall. This apparent anomaly is yet to be explained. The stalling angle of attack however is near  $18^\circ$  over the remainder of the RN range. The (pre-stall) lift curve slope is more or less constant at 0.09 per degree over the RN range studied. This differs from the slope of 0.1 for RN of 3 to 9 million given in Reference 3. Beyond  $18^\circ$  the lift coefficient drops to a local minimum of 0.9 at  $31^\circ$  and then rises to a local maximum of 1.2 (secondary stall) at  $42^\circ$  before dropping off sharply with angle of attack beyond  $46^\circ$ . Further, the effect of the Reynolds number variation is minimal in the angle of attack region beyond the local minimum. In summary, the RN effect on the lift characteristic is noticeable only in and around stall.

POST STALL STUDIES

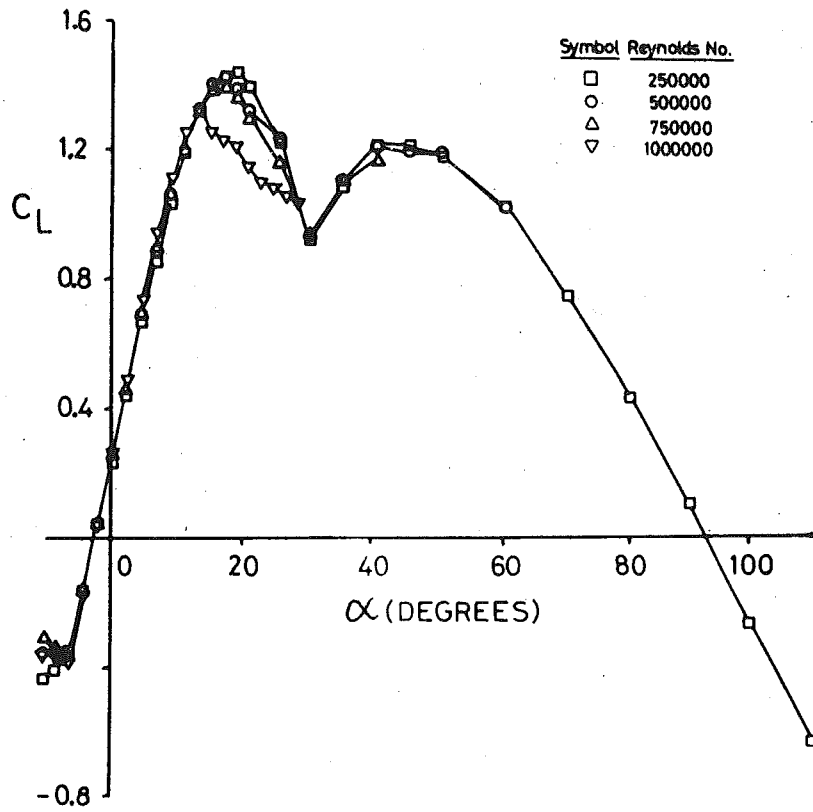


Figure 3 Aerodynamic Coefficients of the NACA 4415 Airfoil, Infinite Aspect Ratio

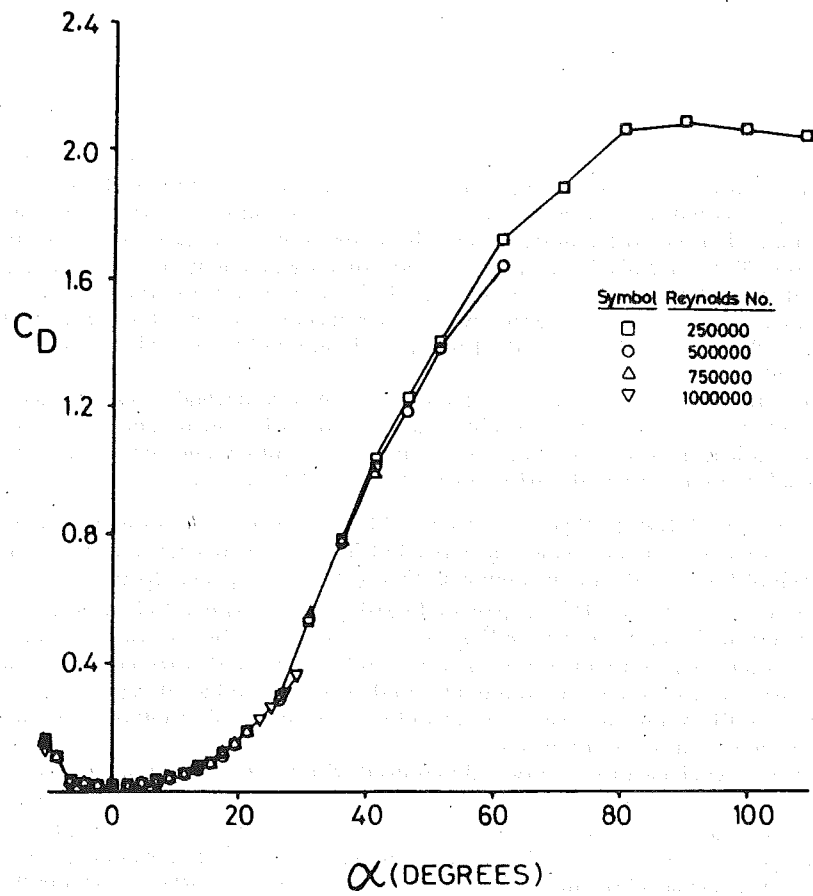


Figure 3 Continued

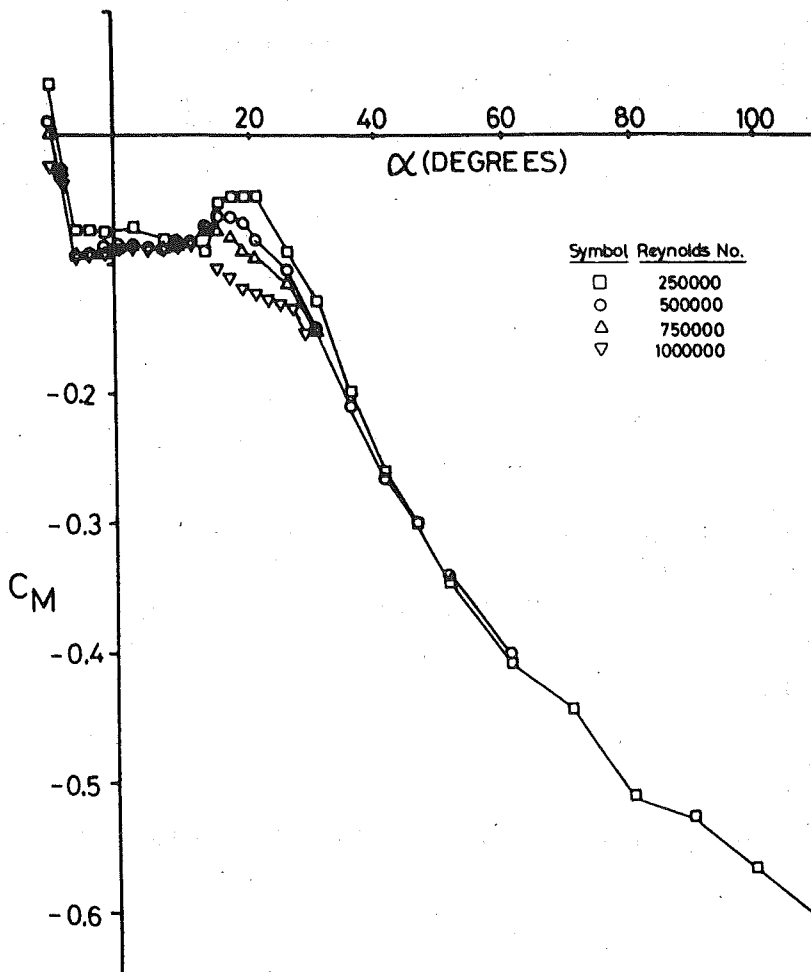


Figure 3 Concluded

There is a rapid rise in drag past  $C_{Lmax}$  (Figure 3(b)). Maximum  $C_D$  is reached at  $\alpha = 90^\circ$ . This maximum value (2.06) is close to the theoretical limit of 2.0 for a two-dimensional flat plate at  $90^\circ$ . The effect of Reynolds number variation on the drag is minimal in the post-stall region but also appears to be insignificant in the pre-stall region. The latter observation is an illusion that arises merely because the large scale, required to depict the entire drag characteristic, scales out the variations at the low drag values. A wake rake survey (performed simultaneously but not presented in this paper) confirmed that the effect of RN variation on the pre-stall drag is fairly pronounced.

The pitching moment curves in Figure 3(c) show a somewhat stable characteristic up to  $\alpha = 10^\circ$ , but a highly unstable characteristic at the higher angles of attack. There is a noticeable RN effect on pitching moment in and beyond the stall region but this effect diminishes with further increase in angle of attack.

**Effect of Aspect Ratio:** In Figures 4 through 7 the effect of aspect ratio variation on the aerodynamic characteristics (specifically lift and drag coefficients) is presented at each of the four Reynolds numbers. Figure 4 shows  $C_L$  and  $C_D$  for AR of  $\infty$ , 12, 9 and 6 at  $RN = 0.25 \times 10^6$ . A general lowering of the lift coefficient curve over the angle of attack range  $-10^\circ$  to  $90^\circ$  is observed to occur with a decrease in aspect ratio. An interesting consequence of the aspect ratio effect is that for combinations of both low aspect ratio and low Reynolds number, the second local maximum (secondary stall) completely disappears and the lift is observed to fall off continuously from a maximum at initial stall.

The drag coefficient is significantly reduced with a decrease in aspect ratio at post stall angles of attack (Figures 4(b), 5(b), 6(b) and 7(b)). In Figure 4(b),  $C_{Dmax}$  has value of 2.06 for an infinite aspect ratio blade and the maximum occurs at an angle of attack of  $90^\circ$ . These trends may be compared with those given in Reference 5 for low aspect ratio wings with Clark-Y airfoil sections at RN of 0.153 million. The lift and drag coefficient curves in Reference 5 are qualitatively similar to those in the present report. In particular, the  $C_{Dmax}$  occurs at  $90^\circ$  and its value falls in the 1.2 to 16. range (larger maximum value for larger aspect ratio).

POST STALL STUDIES

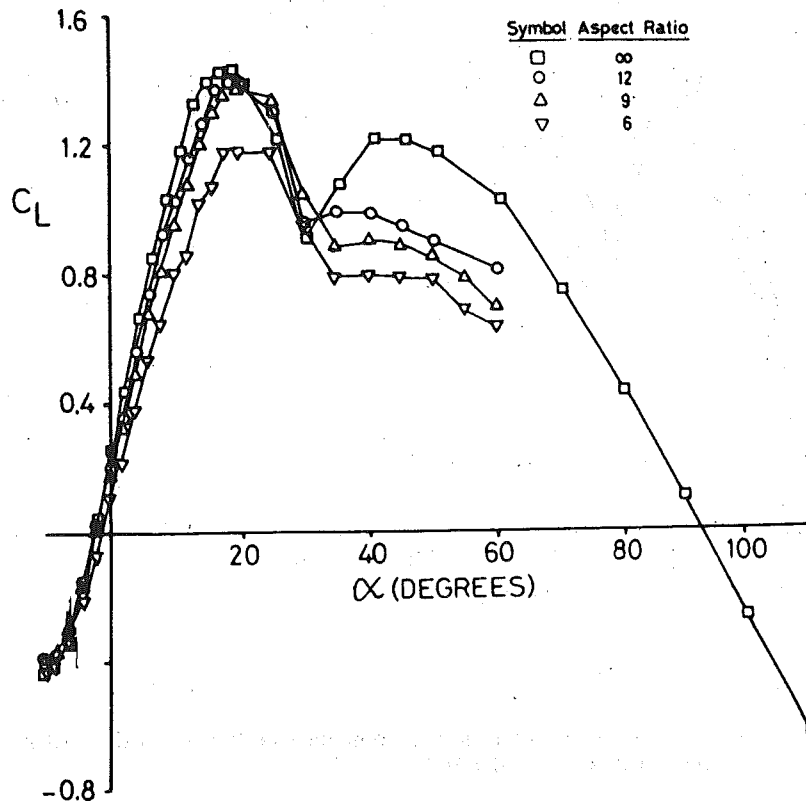


Figure 4 Effect of Aspect Ratio on the Aerodynamic Coefficients of the NACA 4415 Airfoil at  $RN = 0.25 \times 10^6$

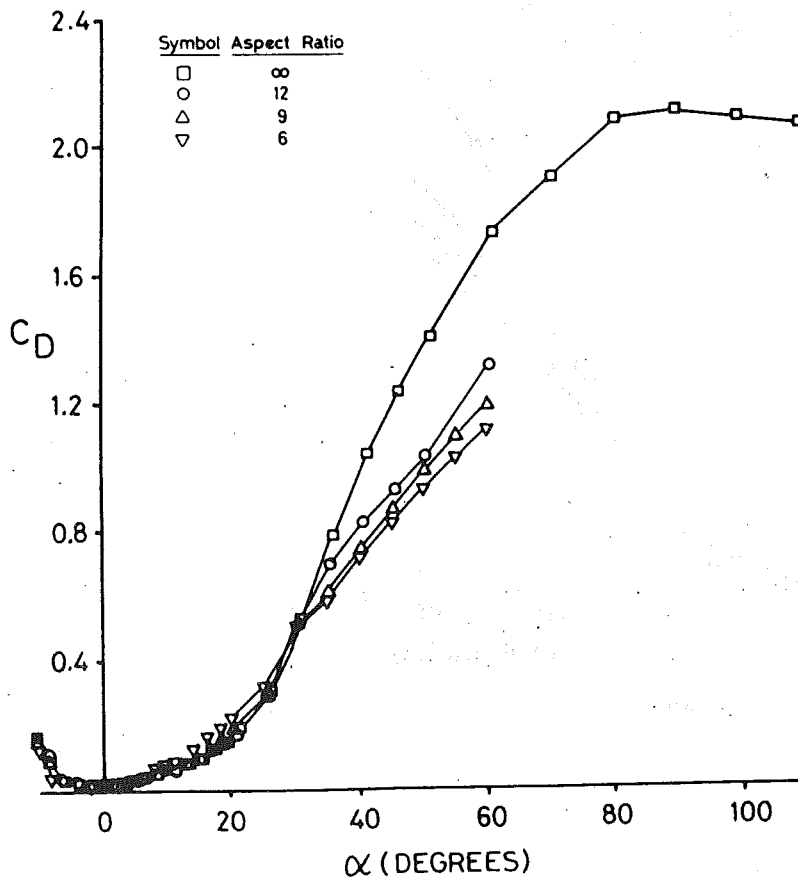


Figure 4 Concluded

POST STALL STUDIES

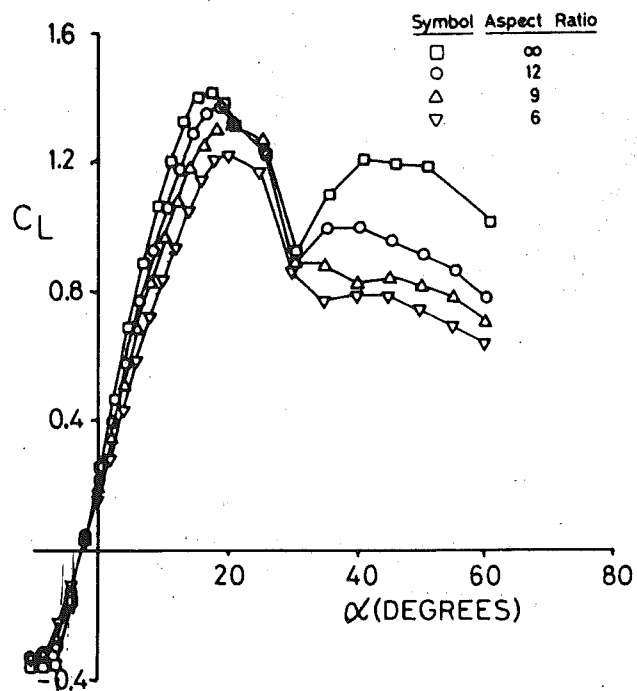


Figure 5 Effect of Aspect Ratio on the Aerodynamic Coefficients of the NACA 4415 Airfoil at  $RN = 0.50 \times 10^6$

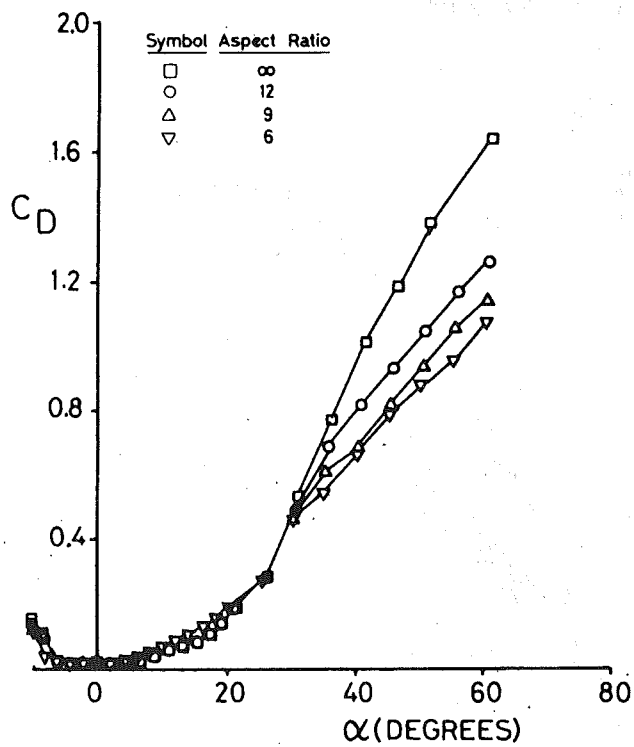


Figure 5 Concluded

POST STALL STUDIES

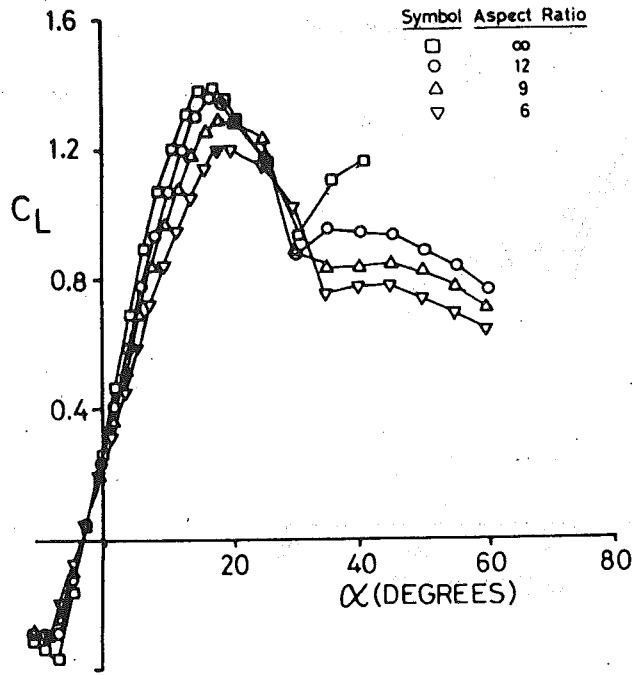


Figure 6 Effect of Aspect Ratio on the Aerodynamic Coefficients of the NACA 4415 Airfoil at  $RN = 0.75 \times 10^6$

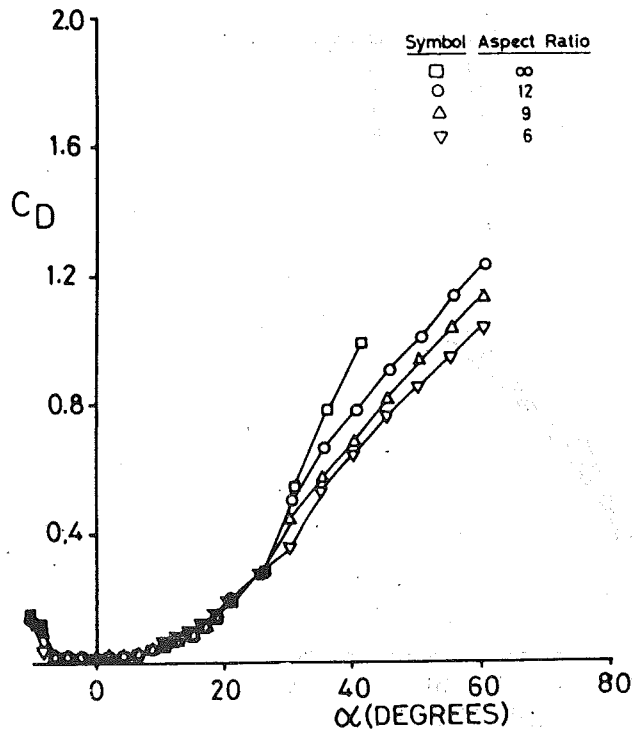


Figure 6 Concluded

POST STALL STUDIES

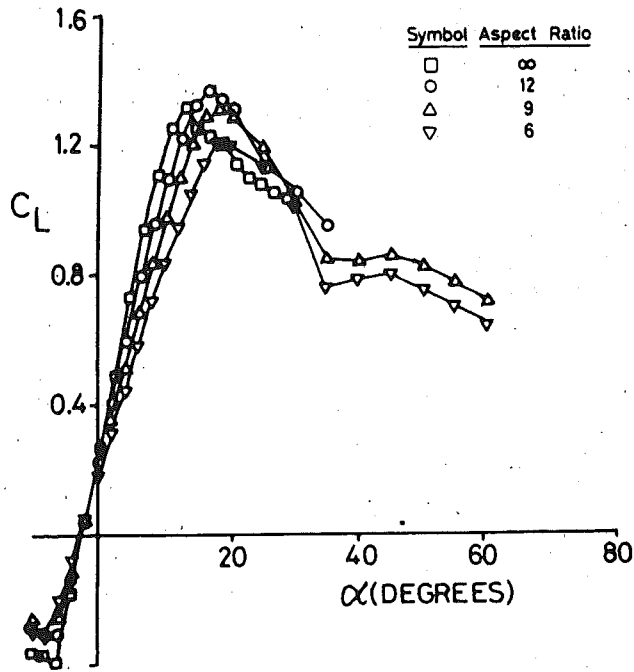


Figure 7 Effect of Aspect Ratio on the Aerodynamic Coefficients of the NACA 4415 Airfoil at  $RN = 1.00 \times 10^6$

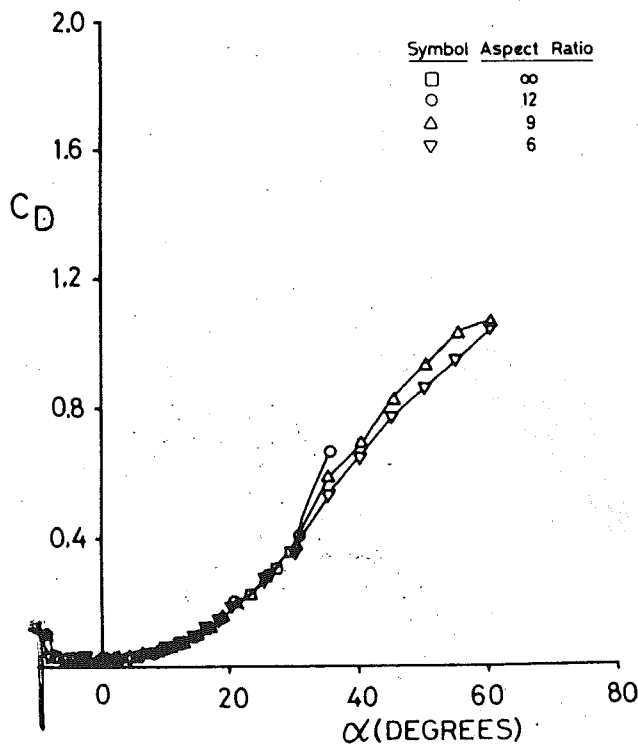


Figure 7 Concluded

## POST STALL STUDIES

**Effect of boundary layer tripping:** The lift and drag characteristics of the blade with boundary layer tripping, along with a comparison with the clean blade, are presented in Figures 8 through 11. Three aspect ratios ( $\infty$ , 12 and 6) were investigated at the four Reynolds numbers given in Table II. The artificial tripping of the boundary layer decreases the lift curve slope by about 5%, lowers  $C_{Lmax}$  and generally lowers the lift curve for angles of attack up to the local minima. These minima (0.9 at  $31^\circ$ ) and the lift curve beyond this point are the same as that for the clean airfoil. Beyond the local minima the lift curve seems unaffected by the tripping. Also, the stalling angle of attack is only marginally affected. The decrease in the lift curve slope is more pronounced at higher RN (Figures 10 and 11).

The drag coefficient of the artificially tripped blade is typically less than or equal to the clean surface value in the post separated region. There is a noticeable decrease in deep stall drag for the lowest aspect ratio. An important point is that in the deep stall region, that is, beyond secondary stall, the characteristics are not critically dependent on the surface cleanliness for the high aspect ratio blades. This is relevant because portions of the wind turbine blades also operate in the deep stall region.

Further, it may be inferred from these figures that, for the blade with artificial tripping, the  $C_{Lmax}$  decreases (and occurs at progressively lower angles of attack) with increasing Reynolds number. This behaviour was observed for the clean airfoil as discussed earlier. For aspect ratios above 6 the post-stall local minimum occurs at  $\alpha = 31^\circ$ . Secondary stall occurs between 40 and 45 degrees.  $C_D$  reaches a maximum at  $\alpha = 90^\circ$ .

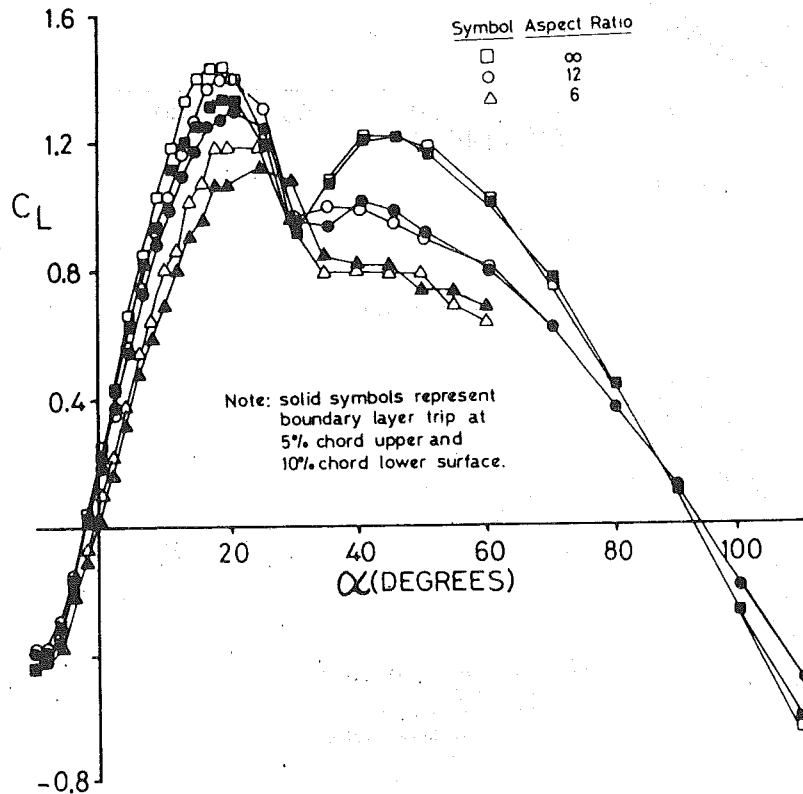


Figure 8 Effect of Boundary Layer Tripping on the Aerodynamic Coefficients of the NACA 4415 Airfoil at  $RN = 0.25 \times 10^6$

POST STALL STUDIES

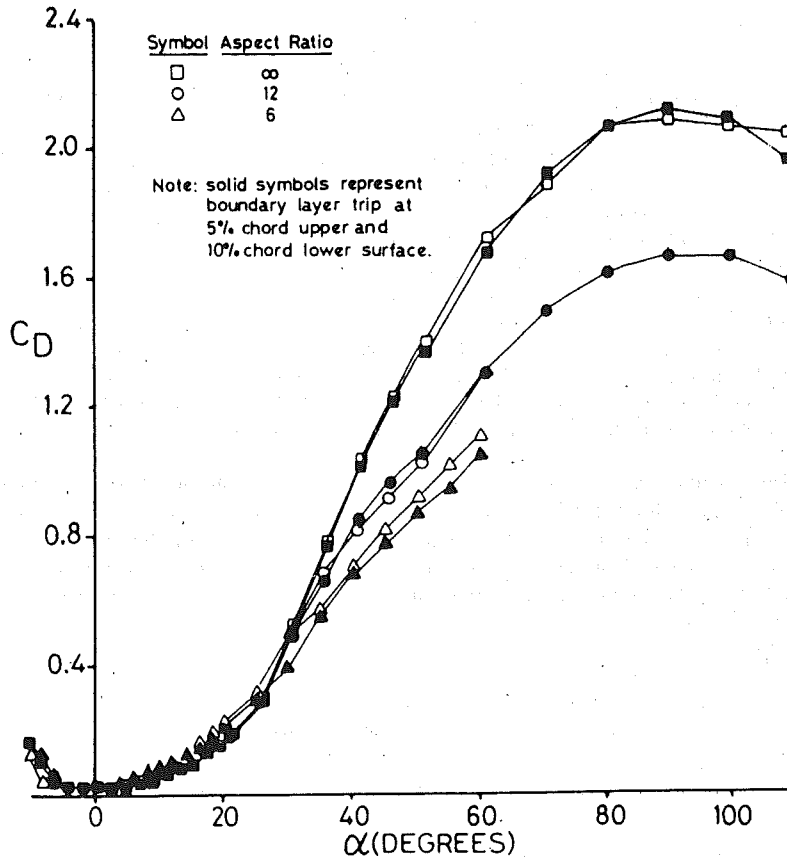


Figure 8 Concluded

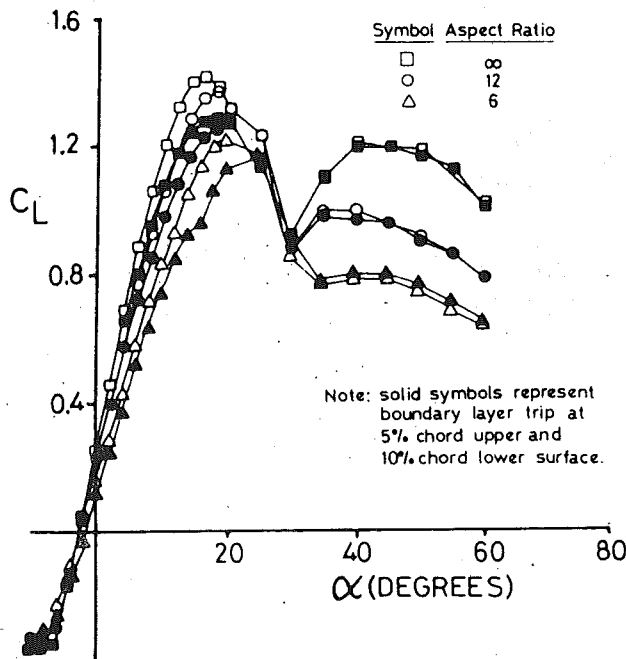


Figure 9 Effect of Boundary Layer Tripping on the Aerodynamic Coefficients of the NACA 4415 Airfoil at  $RN = 0.50 \times 10^6$

POST STALL STUDIES

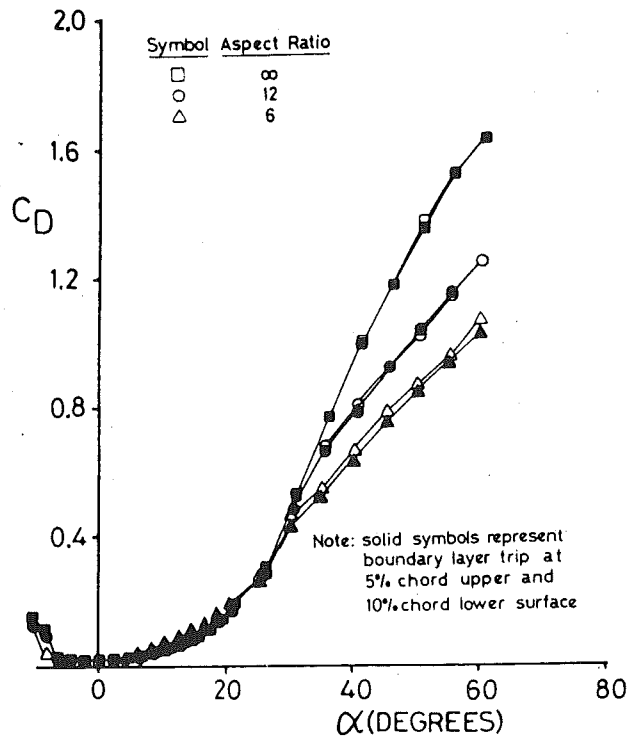


Figure 9 Concluded

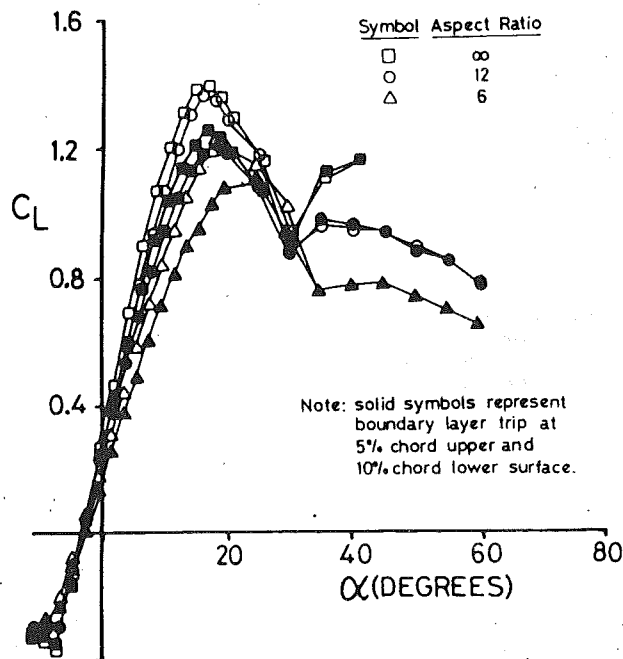


Figure 10 Effect of Boundary Layer Tripping on the Aerodynamic Coefficients of the NACA 4415 Airfoil at  $Re = 0.75 \times 10^6$

POST STALL STUDIES

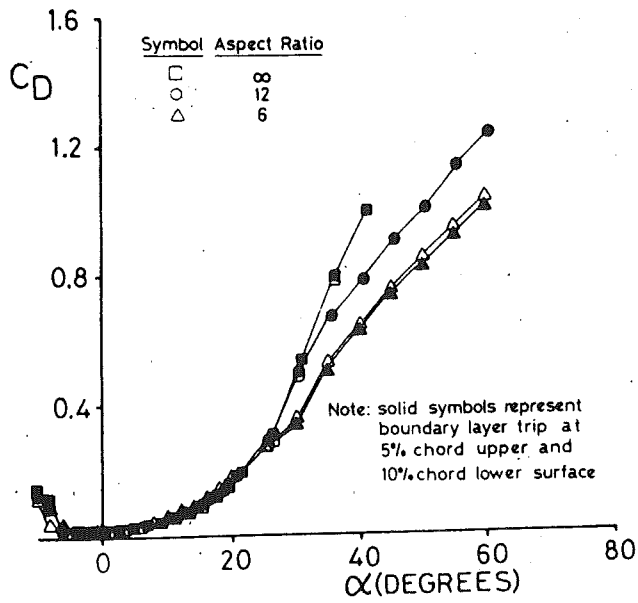


Figure 10 Concluded

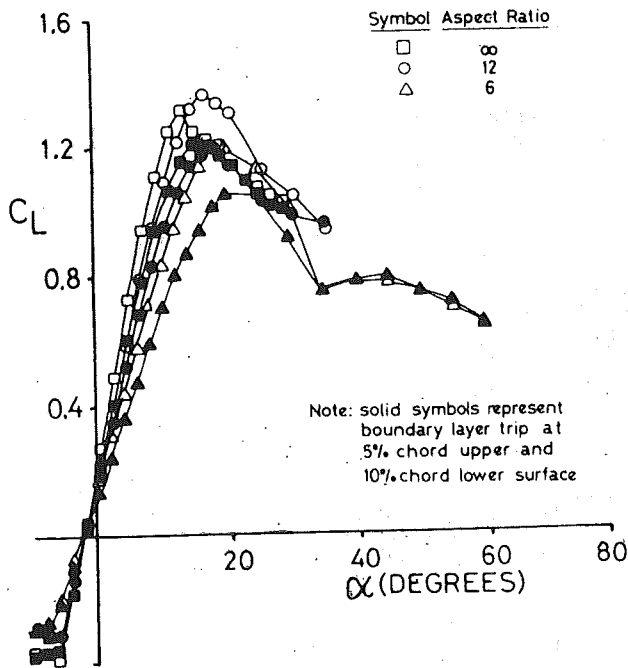


Figure 11 Effect of Boundary Layer Tripping on the Aerodynamic Coefficients of the NACA 4415 Airfoil at  $RN = 1.00 \times 10^6$

POST STALL STUDIES

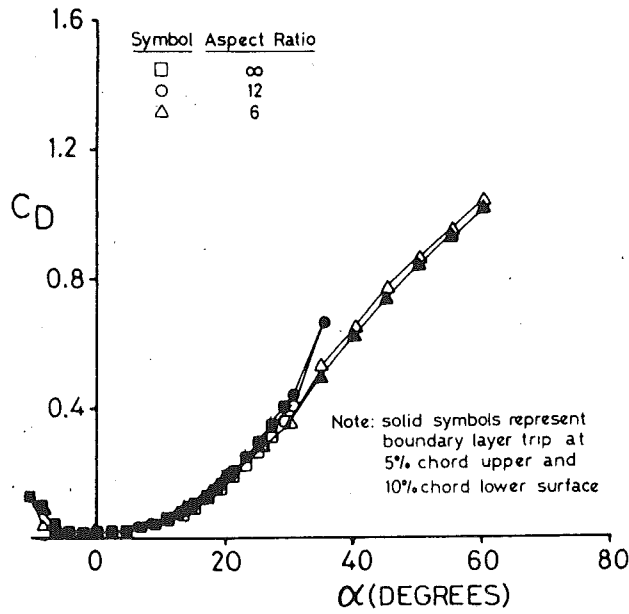


Figure 11 Concluded

**Lift/Drag Characteristic:** The lift to drag ratio is presented, Figures 12 through 15, as a function of angle of attack for the four aspect ratios at each of the four Reynolds numbers. The L/D is independent of aspect ratio in the region beyond secondary stall ( $\alpha > 31^\circ$ ). The L/D characteristic is highly aspect ratio sensitive in the region just before and after primary stall. The maximum L/D for the infinite aspect ratio blade is roughly twice that for an aspect ratio of 6. This seems to be independent of Reynolds number. At low Reynolds number (one quarter million), there is a kink in the curve near maximum L/D. This kink disappears with an increase in Reynolds number.

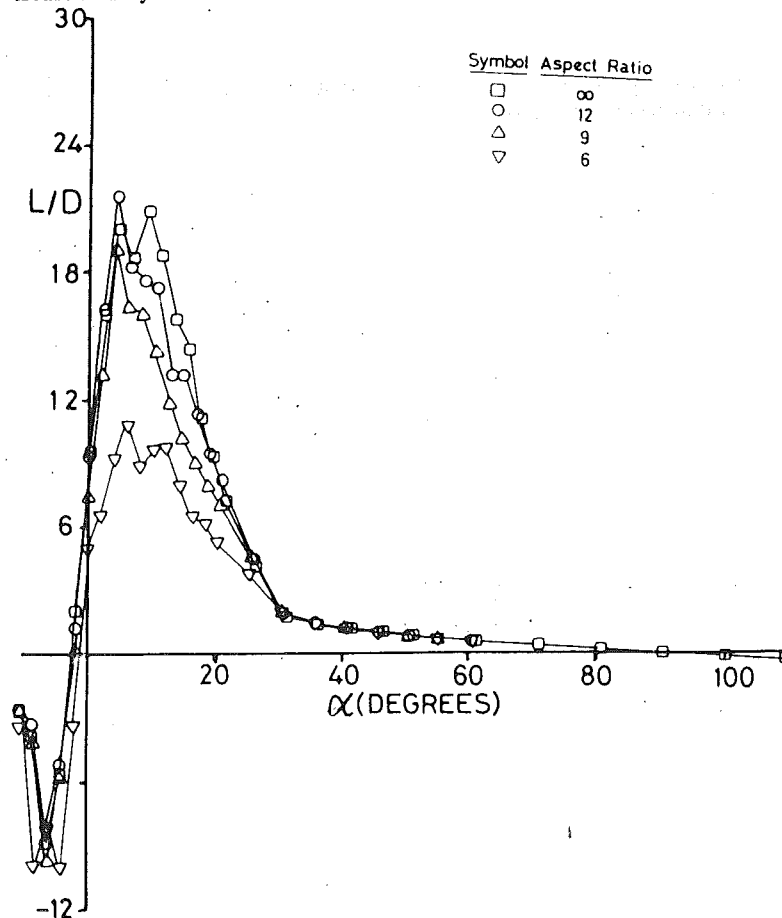


Figure 12 Effect of Aspect Ratio on the Lift to Drag Ratio of the NACA 4415 Airfoil at  $RN = 0.25 \times 10^6$

POST STALL STUDIES

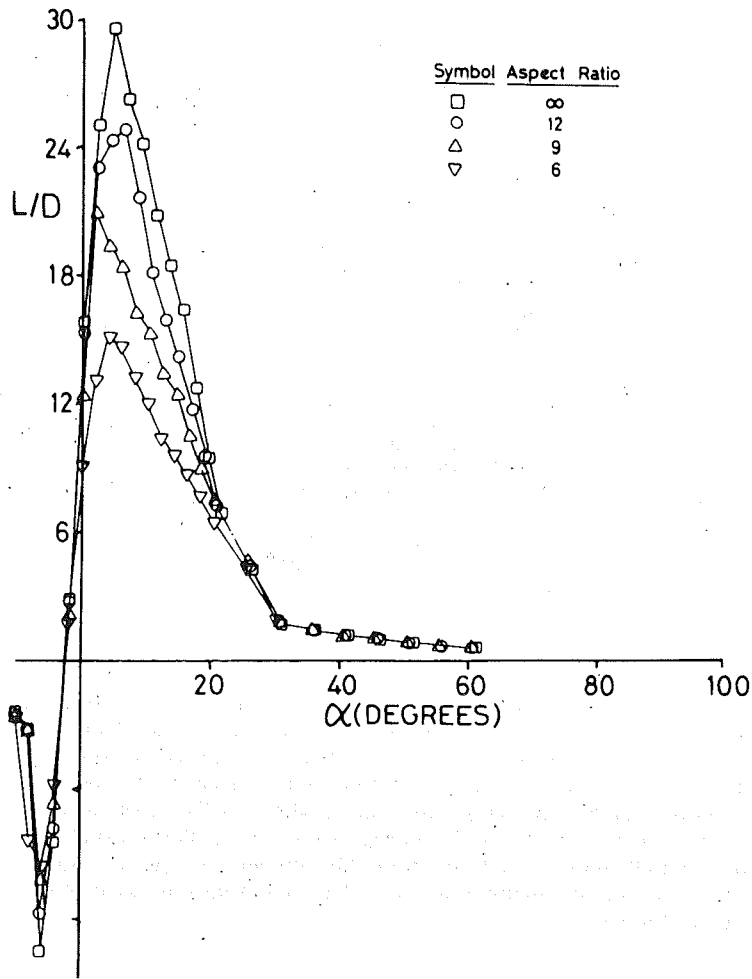


Figure 13 Effect of Aspect Ratio on the Lift to Drag Ratio of the NACA 4415 Airfoil at  $RN = 0.50 \times 10^6$

POST STALL STUDIES

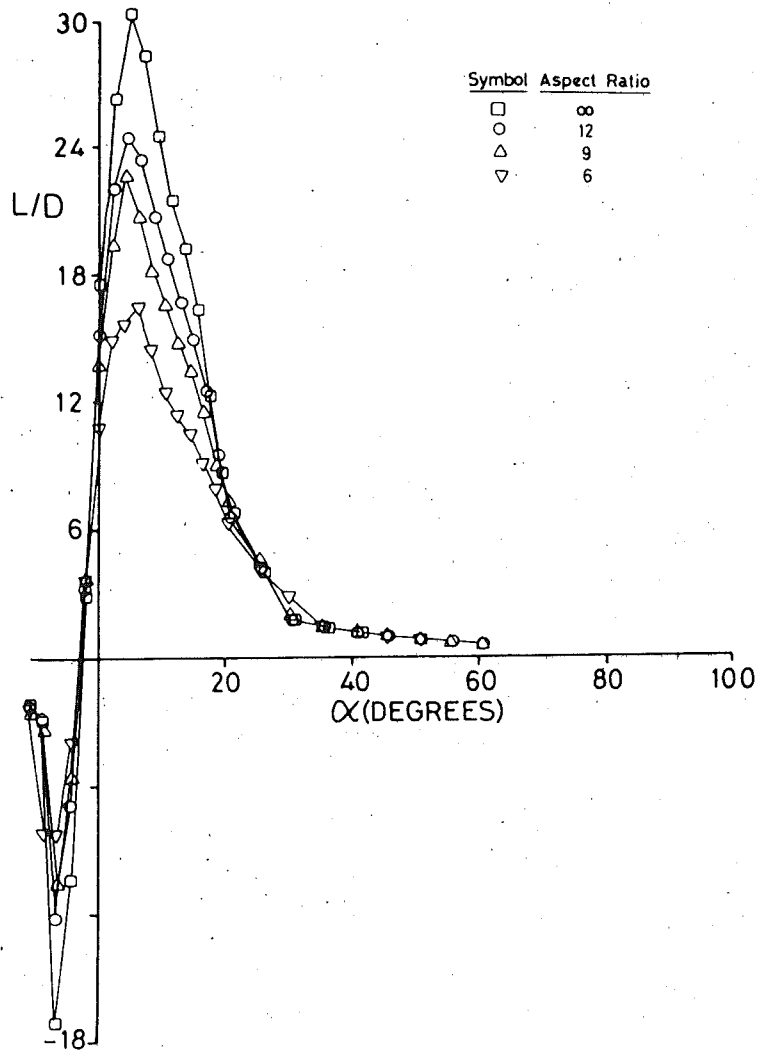


Figure 14 Effect of Aspect Ratio on the Lift to Drag Ratio of the NACA 4415 Airfoil at  $RN = 0.75 \times 10^6$

POST STALL STUDIES

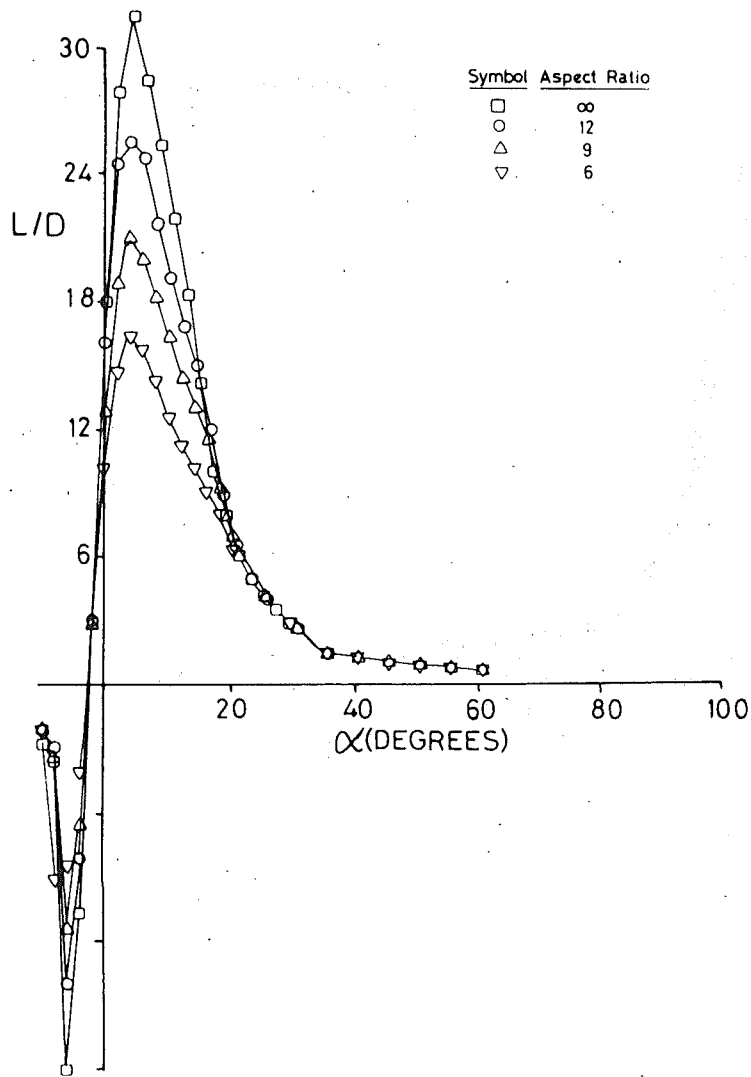


Figure 15 Effect of Aspect Ratio on the Lift to Drag Ratio of the NACA 4415 Airfoil at  $RN = 1.00 \times 10^6$

CONCLUSIONS

Force and moment data are presented for untwisted blades with an NACA 4415 airfoil section with aspect ratios of infinity, 12, 9 and 6 for Reynolds Numbers of 0.25, 0.50, 0.75 and  $1.00 \times 10^6$ . From these data the following conclusions are drawn:

1. In general, the lift coefficient data indicates both initial and secondary stall over the angle of attack range of  $-10^\circ$  to  $110^\circ$ . The maximum drag coefficient occurs at  $90^\circ$ , with the highest value at 2.06 for an infinite aspect ratio blade. The pitching moment is unstable beyond stall.
2. The effect of variation in Reynolds number on the lift and pitching moment characteristics is noticeable only in and around stall. The unexpected increase in maximum lift coefficient with decreasing Reynolds number is attributed to blade bending as a result of the higher dynamic pressures.
3. The lift coefficient decreases with decreasing aspect ratio. For aspect ratios of 9 and 6 secondary stall is eliminated only at Reynolds numbers below one million. The post-stall drag coefficient decreases significantly with a decrease in aspect ratio.
4. Boundary layer tripping is observed to decrease the lift curve slope, the maximum lift coefficient and the stall angle of attack. More importantly, boundary layer tripping does not critically affect the deep stall characteristics.
5. The lift to drag characteristic is independent of aspect ratio beyond secondary stall but is highly aspect ratio sensitive just in and around primary stall. For the Reynolds number range studied, the maximum lift to drag ratio for the infinite aspect ratio blade is twice that for a blade with an aspect ratio of 6.

ACKNOWLEDGEMENT

The authors wish to express their appreciation for the support of this work by Rockwell International, especially Mr. J. Tangler of the Wind Energy Research Staff.

REFERENCES

1. Michos, A., Bergeles, G. and Athanassiadis, N. *Aerodynamic Characteristics of NACA 0012 Airfoil in Relation to Wind Generators, Wind Engineering, Vol. 7, No. 4, 1983, pp. 247-262.*
2. Snyder, M.H. and Satran, D. *Two-Dimensional Tests of GA(W)-1 and GA(W)-2 Airfoils at Angles of Attack from 0 to 360 Degrees, WER-1, Wind Energy Laboratory, Wichita State University, Wichita, Kansas, January, 1977.*
3. Abbott, I.H. and Von Doenhoff, A.E. *Theory of Wing Sections, Dover Publications, Inc., New York, 1959, pp. 488-493.*
4. Pope, A. and Harper, J.J. *Low-Speed Wind Tunnel Testing, John Wiley & Sons, New York, New York, 1966.*
5. Knight, M. and Wenzinger, C.J. *Wind Tunnel Tests on a Series of Wing Models through a Large Angle of Attack Range Part I - Force Tests, NACA TR 317, 1929.*